

Coupled map car-following model and its delayed-feedback control

Keiji Konishi,* Hideki Kokame, and Kentaro Hirata

Department of Electrical and Electronic Systems, Osaka Prefecture University, 1-1 Gakuen-cho, Sakai, Osaka 599-8531, Japan

(Received 20 April 1999)

This paper proposes a coupled map car-following traffic model, which describes a dynamical behavior of a group of road vehicles running in a single lane without overtaking. This model consists of a lead vehicle and following vehicles, which have a piecewise linear optimal velocity function. When the lead-vehicle speed is varied, we can observe a traffic jam in the group of the vehicles. We derive a condition under which the traffic jam never occurs in our model. Furthermore, in order to suppress the traffic jam, for each vehicle we use a dynamic version of decentralized delayed-feedback control proposed in [Konishi, Hirai, and Kokame, Phys. Rev. E **58**, 3055 (1998)], and provide a systematic procedure for designing the controller. [S1063-651X(99)12410-3]

PACS number(s): 05.45.-a

I. INTRODUCTION

The idea of controlling chaos has been widely investigated in the field of nonlinear dynamics [1]. Ott, Grebogi, and Yorke (OGY) gave a method (the OGY method), which stabilizes chaotic motions onto a desired unstable periodic orbit (UPO) within a chaotic attractor [2]. Pyragas proposed a delayed-feedback control (DFC) method, which does not require a reference signal corresponding to the desired UPO [3]. The DFC method was successfully applied to several physical systems [1], since it is a practical scheme for stabilizing real chaotic systems. Furthermore, several researchers analyzed the stability of the DFC system [4–7], and discussed a discrete-time version [8–13] of the method. Most of these studies dealt with the stabilization of temporal chaos in low-dimensional systems; on the contrary, investigations of spatiotemporal chaotic behavior and its control have attracted much interest recently [14]. Konishi, Hirai, and Kokame [15] proposed a decentralized delayed-feedback control (DDFC) for a one-way coupled open map lattice [16,17]. They derived a necessary and sufficient condition for the decentralized delayed-feedback control system to be stable. The paper [15] gave a simple procedure for designing the robust local controllers.

In recent years, the traffic flow problems have been widely investigated in the field of physics [18–32]. In order to understand the phenomena in traffic flow, several traffic flow models have been proposed: coupled differential equation models [18–25], coupled map models [26–28], and cellular automata [29–32]. Bando *et al.* proposed a simple car-following model, which is called the optimal velocity (OV) model [18]. Each vehicle of this model is described by a simple differential equation. The vehicle equation uses the OV function, which provides the optimal velocity depending on the headway distance: each driver controls the velocity based on the OV function. The paper [18] showed traffic jam phenomena under periodic boundary conditions, and derived

a simple stability condition of the OV model. Komatsu and Sasa studied the traffic jam on the OV model in detail [19]. The OV model was modified from several view points: delay effect [20–22], modification to be simple and solvable [23], and generalization of the model [24].

On the other hand, the coupled map (CM) traffic models were proposed to show several traffic phenomena on computer simulations [26–28]. The CM traffic models have continuous state variables, discrete time, and discrete space. Although the large scale OV model takes a long time to analyze its behavior due to huge numerical integration, the CM traffic models do not take a long time for computer simulation because of its simple time-development algorithm. The CM traffic models can be divided into two types. One of them is the chaotic CM traffic model [26,27]: each vehicle shows chaotic behavior, since its OV function is set as a chaotic map. Another model is a nonchaotic CM model that is a discrete-time version of the original OV model [28]: each vehicle does not behave chaotically, since its OV function is similar to that of the original OV model. The paper [28] investigated effects of noises under open boundary bottlenecks on computer simulations; however, no studies have ever tried to analyze theoretically the traffic jam in the CM model.

Although most of the papers related to the OV and CM models have investigated the mechanism of the traffic jam phenomena, to our knowledge, there are no studies on suppression of the phenomena. The suppression must be an important subject of urban road traffic flow. The present paper has two purposes: (i) we analyze theoretically the traffic jam phenomena in a simple CM traffic model and (ii) we propose a scheme for suppression of the traffic jam. On the basis of the paper [28], the present paper introduces a coupled map car-following traffic model, which describes the dynamical behavior of a group of road vehicles running in a single lane without overtaking. Our model consists of a lead vehicle and following vehicles which have a piecewise linear optimal velocity function. We derive a simple sufficient condition under which the traffic jam never occurs in the vehicle group. Furthermore, in order to suppress the traffic jam, we utilize a dynamical version of the decentralized delayed-feedback control scheme proposed in [15] for each

*Author to whom correspondence should be addressed.

FAX: +81-722-54-9907. Electronic address:

konishi@ecs.ees.osakafu-u.ac.jp

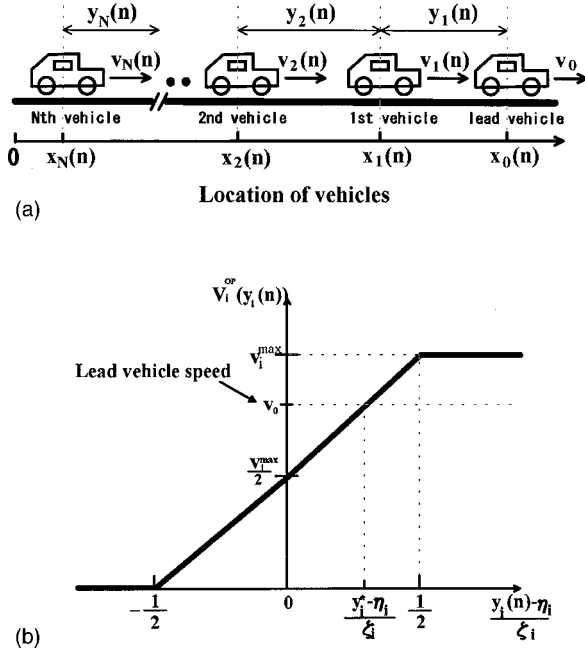


FIG. 1. Illustrations of car-following model and piecewise linear optimal velocity function. (a) Car-following model. (b) Piecewise linear optimal velocity function.

vehicle, and provide a systematic procedure for designing the controller. Some numerical examples are shown to confirm the theoretical results.

This paper is organized as follows. Section II proposes a coupled map car-following traffic model and analyzes its stability. In Sec. III, the dynamical version of the decentralized delayed-feedback control scheme is introduced for suppression of the traffic jam in the model, and we give a simple procedure for designing the controller. Finally, conclusions are presented in Sec. IV.

II. COUPLED MAP CAR-FOLLOWING MODEL

A. Description of traffic model

Let us consider a coupled map car-following traffic model illustrated in Fig. 1(a). The lead vehicle is described as

$$x_0(n+1) = v_0 T + x_0(n), \quad (1)$$

where $x_0(n) > 0$ is the position of the leading vehicle at time $t = nT$, $v_0 > 0$ is its speed, and $T > 0$ is the sampling time. We assume that the lead vehicle is not influenced by others. The following vehicles are given as

$$x_i(n+1) = v_i(n)T + x_i(n) \quad (i = 1 \sim N), \quad (2)$$

where $x_i(n) > 0$ is the position of the i th vehicle, $v_i(n) > 0$ is the i th vehicle speed, and N is the number of the following vehicles. The speed of the following vehicles is governed by

$$v_i(n+1) = \alpha_i [V_i^{\text{op}}(y_i(n)) - v_i(n)]T + v_i(n). \quad (3)$$

$\alpha_i > 0$ is the sensitivity of the i th vehicle driver. $V_i^{\text{op}}(y_i(n))$ is the OV function, which depends only on a headway distance $y_i(n)$ between the $(i-1)$ th and i th vehicles:

$$y_i(n) = x_{i-1}(n) - x_i(n). \quad (4)$$

For simplicity, this paper adopts the following piecewise linear function as the OV function:

$$V_i^{\text{op}}(y_i(n)) = \frac{v_i^{\text{max}}}{2} \left[1 + \bar{H}_{\text{sat}} \left(2 \frac{y_i(n) - \eta_i}{\zeta_i} \right) \right], \quad (5)$$

where the saturation function, $\bar{H}_{\text{sat}}(\cdot)$ is described as

$$\bar{H}_{\text{sat}}(\rho) = \begin{cases} +1 & \text{if } \rho < -1 \\ \rho & \text{if } -1 \leq \rho \leq +1 \\ -1 & \text{if } \rho > +1 \end{cases} \quad (6)$$

$v_i^{\text{max}} > 0$ is the maximum speed, $\eta_i > 0$ is the neutral headway distance, and $\zeta_i > 0$ is the parameter. Figure 1(b) sketches the piecewise linear OV function. We assume that the lead vehicle speed v_0 is less than the maximum speed of all the following vehicles, i.e.,

$$v_0 < v_i^{\text{max}} \quad (i = 1, 2, \dots, N). \quad (7)$$

This assumption guarantees an existence of a vehicle group. If one vehicle of the group does not satisfy this assumption, this vehicle cannot follow the preceding vehicle. As a result, this vehicle becomes a new lead vehicle of the second group.

To avoid the collisions and backward motions, all the vehicles adopt the full-braking action:

$$\begin{aligned} \text{if } y_i(n) < y_i^{\text{min}}, \quad \text{then } x_i(n+1) &= x_i(n) \\ \text{and } v_i(n+1) &= 0. \end{aligned} \quad (8)$$

This action implies that the i th vehicle stops suddenly when the headway distance $y_i(n)$ is less than a minimum distance y_i^{min} .

B. Stability analysis

A vehicle behavior depends only on the headway distance; hence, our car-following model can be reduced to a simple system. If the preceding vehicle [i.e., $(i-1)$ th vehicle] runs with the lead-vehicle speed v_0 , then the dynamics of the i th vehicle can be given as

$$\begin{aligned} v_i(n+1) &= \alpha_i [V_i^{\text{op}}(y_i(n)) - v_i(n)]T + v_i(n), \\ y_i(n+1) &= v_0 T - v_i(n)T + y_i(n). \end{aligned} \quad (9)$$

The steady state of system (9) is

$$[v_i^* \quad y_i^*]^T = \left[v_0 \frac{v_0}{r_i} - \frac{\zeta_i}{2} + \eta_i \right]^T, \quad (10)$$

where $r_i = v_i^{\text{max}}/\zeta_i$. It is clear that the necessary and sufficient condition for the existence of steady state (10) is condition (7) [see also, Fig. 1(b)]. Let us consider an error system around steady state (10):

TABLE I. Parameters for numerical simulations.

Parameter	Value	Unit
η	25.0	m
ζ	23.3	m
v^{\max}	33.6	m/sec
α	2.0	sec ⁻¹
T	0.1	sec
y^{\min}	7.02	m

$$\begin{bmatrix} \delta v_i(n+1) \\ \delta y_i(n+1) \end{bmatrix} = \begin{bmatrix} 1 - \alpha_i T & \alpha_i r_i T \\ -T & 1 \end{bmatrix} \begin{bmatrix} \delta v_i(n) \\ \delta y_i(n) \end{bmatrix}, \quad (11)$$

where $\delta v_i(n) = v_i(n) - v_i^*$ and $\delta y_i(n) = y_i(n) - y_i^*$. The stability of steady state (10) depends only on system matrix (11). The characteristic polynomial of system (11) is

$$P_i(z) = z^2 + a_i z + b_i, \quad (12)$$

where $a_i = \alpha_i T - 2$ and $b_i = 1 - \alpha_i T + \alpha_i r_i T^2$. Jury scheme allows us to derive a necessary and sufficient condition for system (11) to be stable. The condition is summarized as the following lemma.

Lemma 1. Linear system (11) is stable if and only if

$$0 < r_i < \frac{1}{T}, \quad 0 < \alpha_i < \frac{4}{(2 - r_i T)T}. \quad (13)$$

Condition (13) means that all the roots of $P_i(z) = 0$ are within a unit circle. Lemma 1 implies that the i th vehicle satisfying condition (13) can run with the lead-vehicle speed v_0 when the preceding vehicle [i.e., $(i-1)$ th vehicle] is running constantly with v_0 .

C. Numerical simulations

We simulate our traffic flow model on the computer. Let us consider a situation where the lead vehicle stops suddenly for a short time:

$$x_0(n) = 0 \quad \text{for } n_s \leq n \leq n_e. \quad (14)$$

This short stop can be considered as a kind of external disturbance for our traffic model. The parameters used in our simulations are given in Table I. All parameters were used in paper [28]. For simplicity, we assume that all vehicles have the same parameters. From Lemma 1 we can see that each vehicle is stable when the preceding vehicle is running at the same speed of the lead vehicle [i.e., the parameters in Table I satisfy condition (13)]. The initial positions and speeds are set as

$$x_i(0) = \sum_{j=i+1}^N y_j^*, \quad y_i(0) = y_i^*, \quad v_i(0) = v_i^* \quad (15)$$

for $i=0, 1, \dots, N$. This initial condition is the steady state of our model. The model runs without the external disturbance

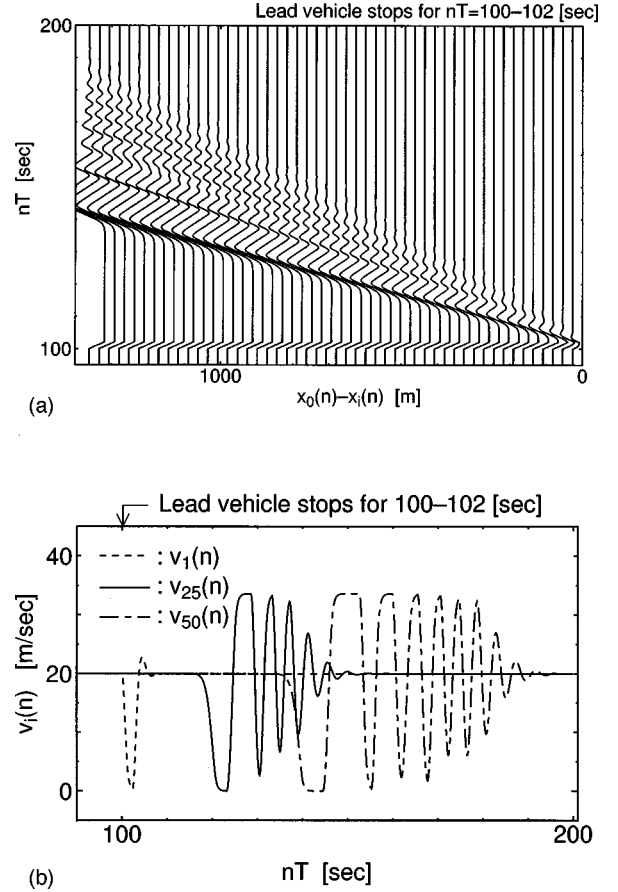


FIG. 2. Numerical simulations for the free-running traffic model. (a) Space-time plot of the free-running traffic model. (b) Temporal velocity behavior of three vehicles.

for $0 \leq n < 1000$ (i.e., $0 \leq nT < 100$ [sec]). The lead vehicle suddenly stops for a short time ($n_s T = 100$, $n_e T = 102$ [sec]). Figure 2(a) shows the space-time plot of the running traffic flow model after $nT = 90$ [sec]. The horizontal axis represents a distance between the lead vehicle and a following vehicle. It can be seen that the stop disturbance propagates the backward vehicles. Figure 2(b) is the temporal velocity of the first, 25th, and 50th vehicles. The stop-time intervals and the transient time of the vehicles increase with vehicle number i . From the above numerical simulations, we notice that even if the stability condition of Lemma 1 is satisfied, the traffic jam occurs in our model. This is because the traffic jam would occur by the following reason: the transient behavior of each vehicle propagates backward with the increase in its amplitude. In order to derive the condition under which the traffic jam never occurs, we shall focus on the transfer function of each vehicle.

D. Nonjam condition

When the preceding vehicle [i.e., $(i-1)$ th vehicle] is not running constantly with v_0 , error system (11) around steady state (10) can be rewritten as

$$\begin{aligned} \begin{bmatrix} \delta v_i(n+1) \\ \delta y_i(n+1) \end{bmatrix} &= \begin{bmatrix} 1 - \alpha_i T & \alpha_i r_i T \\ -T & 1 \end{bmatrix} \begin{bmatrix} \delta v_i(n) \\ \delta y_i(n) \end{bmatrix} + \begin{bmatrix} 0 \\ T \end{bmatrix} \delta v_{i-1}(n), \\ \delta v_i(n) &= [1 \quad 0] \begin{bmatrix} \delta v_i(n) \\ \delta y_i(n) \end{bmatrix}. \end{aligned} \quad (16)$$

The transfer function from $\delta v_{i-1}(n)$ to $\delta v_i(n)$ is described by

$$G_i(z) = [1 \quad 0] \begin{bmatrix} z^{-1} + \alpha_i T & -\alpha_i r_i T \\ T & z - 1 \end{bmatrix}^{-1} \begin{bmatrix} 0 \\ T \end{bmatrix} = \frac{\alpha_i r_i T^2}{P_i(z)}. \quad (17)$$

Since the traffic jam would occur by the increase in amplitude of each-vehicle transient behavior, we have to derive the condition under which the amplitude of the transient behavior decreases. This condition can be reduced to

$$\max_{|z|=1} |G_i(z)| \leq 1 \quad (i = 1, 2, \dots, N). \quad (18)$$

This means that H_∞ norms of all the vehicles are 1 or less. Theorem 1 shows a simple sufficient condition of Eq. (18).

Theorem 1. Assuming that all the vehicles satisfy the condition of Lemma 1, condition (18) holds if the following condition is satisfied:

$$\frac{8 + \alpha_i T (\alpha_i T - 8)}{\alpha_i T^2 (\alpha_i T - 6)} \leq r_i \leq \frac{\alpha_i}{2 + \alpha_i T}. \quad (19)$$

(Proof). See Appendix A.

Figure 3 illustrates the nonjam condition of Theorem 1 on a r_i - α_i plane. Figure 4 shows the space-time plots of our traffic model with three types of driver sensitivity ($\alpha_i = 1.0, 3.0,$ and 6.0). Other parameters are the same as Fig. 2. Since the parameters used in Figs. 4(a)–4(c) satisfy condition (13) of Lemma 1, each vehicle has a stable solution. Figure 4(a) shows a terrible traffic jam in the following vehicles. On the other hand, in Fig. 4(b), we can see the oscillating behavior of vehicles, but cannot observe the terrible traffic jam. The parameters used in Fig. 4(c) satisfy the nonjam condition of Theorem 1; then the influence of the lead-vehicle stop decreases with the number of the vehicle. From these numeri-

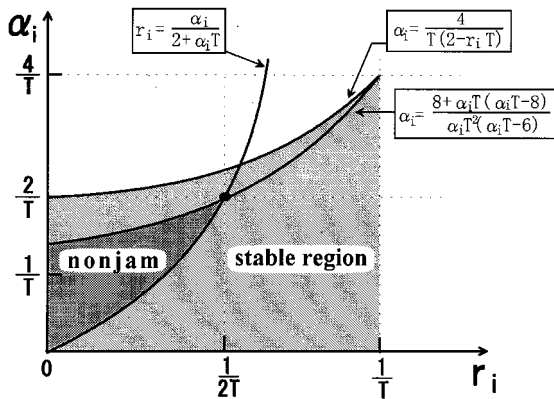


FIG. 3. Nonjam condition on a r_i - α_i plane.

cal simulations, we confirm that the traffic jam never occurs when all the vehicles satisfy the condition of Theorem 1. The next section shall consider how to suppress the traffic jam by the decentralized delayed-feedback control.

III. DELAYED-FEEDBACK CONTROL OF TRAFFIC MODEL

A. Control system

The second purpose of this paper is to propose a control scheme for suppression of traffic jam in our model. Let us add a control signal term to system (3), i.e.,

$$v_i(n+1) = \alpha_i [V_i^{\text{op}}(y_i(n)) - v_i(n)]T + v_i(n) + u_i(n). \quad (20)$$

We adopt a dynamic version of the decentralized delayed-feedback control proposed in [15] as follows:

$$\begin{aligned} w_i(n+1) &= k_i^a w_i(n) + k_i^b [v_i(n) - v_i(n-1)], \\ u_i(n) &= k_i^c w_i(n) + k_i^d [v_i(n) - v_i(n-1)], \end{aligned} \quad (21)$$

where $k_i^a, k_i^b, k_i^c, k_i^d \in \mathbf{R}$ are the feedback gains. The closed-loop system consisting of Eqs. (2), (4), (20), and (21) has the same steady state as system (9). Around steady state (10) the closed-loop system can be described by

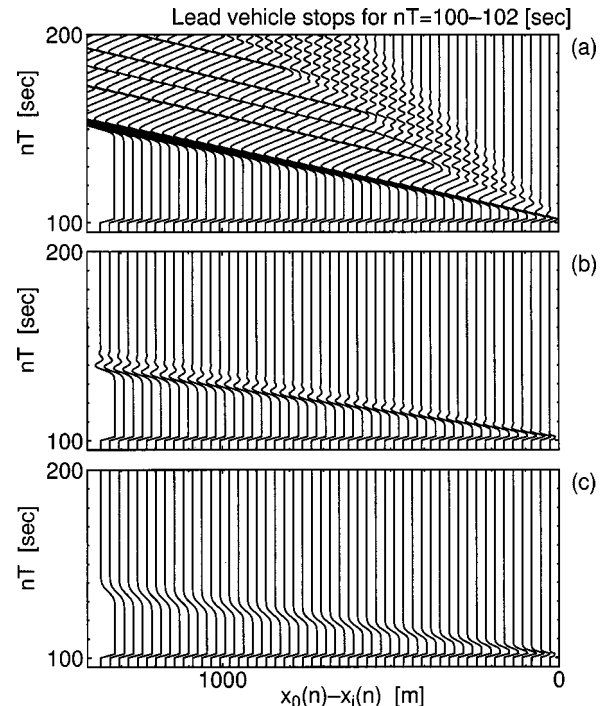


FIG. 4. Numerical simulation of the free-running traffic model with three types of driver sensitivity. (a) $\alpha_i = 1.0$, (b) $\alpha_i = 3.0$, and (c) $\alpha_i = 6.0$.

$$\begin{aligned} \mathbf{q}_i(n+1) &= \mathbf{A}_i \mathbf{q}_i(n) + \mathbf{B} \delta v_{i-1}(n), \\ \delta v_i(n) &= \mathbf{C} \mathbf{q}_i(n), \end{aligned} \quad (22)$$

where

$$\begin{aligned} \mathbf{q}_i(n) &= [\delta v_i(n) \quad \delta v_i(n-1) \quad \delta y_i(n) \quad w_i(n)]^T, \\ \mathbf{A}_i &= \begin{bmatrix} 1 - \alpha_i T + k_i^d & -k_i^d & \alpha_i r_i T & k_i^c \\ 1 & 0 & 0 & 0 \\ -T & 0 & 1 & 0 \\ k_i^b & -k_i^b & 0 & k_i^a \end{bmatrix}, \quad \mathbf{B} = \begin{bmatrix} 0 \\ 0 \\ T \\ 0 \end{bmatrix}, \\ \mathbf{C} &= [1 \quad 0 \quad 0 \quad 0]. \end{aligned}$$

The transfer function from $\delta v_{i-1}(n)$ to $\delta v_i(n)$ is

$$\bar{G}_i(z) = \mathbf{C}(z\mathbf{I}_{4 \times 4} - \mathbf{A}_i)^{-1} \mathbf{B} = \frac{N_i(z)}{D_i(z)}, \quad (23)$$

where

$$\begin{aligned} N_i(z) &= \alpha_i r_i T^2 z(z - k_i^a), \\ D_i(z) &= z^4 + (\alpha_i T - 2 - k_i^a - k_i^d) z^3 + \{\alpha_i r_i T - \alpha_i T(k_i^a + 1) \\ &\quad + 2(k_i^a + k_i^d) + 1 + k_i^a k_i^d - k_i^b k_i^c\} z^2 + \{\alpha_i k_i^a T(1 - r_i T) \\ &\quad - k_i^a - k_i^d + 2(k_i^b k_i^c - k_i^a k_i^d)\} z + k_i^a k_i^d - k_i^b k_i^c. \end{aligned}$$

In order to suppress the traffic jam in our model, we have to design the feedback gains $k_i^a, k_i^b, k_i^c, k_i^d$ such that

$$\max_{|z|=1} |\bar{G}_i(z)| \leq 1 \quad (i = 1, 2, \dots, N). \quad (24)$$

The following theorem provides a systematic procedure on how to design the feedback gains.

Theorem 2. Assume that all the vehicles satisfy the following conditions:

$$-1 < \frac{r_i T(3 - \alpha_i r_i T^2) - 1}{1 - 2r_i T} < +1, \quad (25)$$

$$\frac{r_i^2 T^2 (1 - 2\alpha_i T + 3\alpha_i r_i T^2)^2}{(2 - 5r_i T + \alpha_i r_i^2 T^3)^2} \leq 1. \quad (26)$$

If the feedback gains are set as

$$\begin{aligned} k_i^a &= \frac{\alpha_i T(1 - r_i T) - 1}{\alpha_i T(1 - 2r_i T)}, \quad k_i^b = \frac{\{\alpha_i T(1 - r_i T) - 1\}^3}{\alpha_i^2 T^2 (1 - 2r_i T)^2}, \\ k_i^c &= 1, \quad k_i^d = \frac{\{\alpha_i T(1 - r_i T) - 1\}^2}{\alpha_i T(1 - 2r_i T)}, \end{aligned} \quad (27)$$

then condition (24) is satisfied.

(*Proof.*) See Appendix B.

This theorem provides us with the ability to design the feedback gains to suppress the traffic jam in our model. From this theorem we can obtain a systematic procedure to design the gains: (i) If condition (25) is satisfied, then go to the next step; otherwise, go to exist. (ii) If condition (26) is

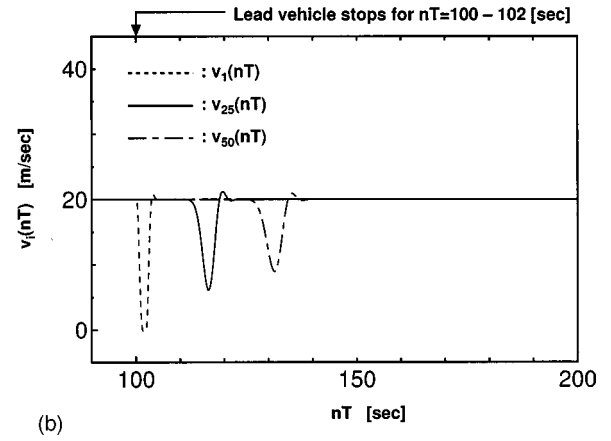
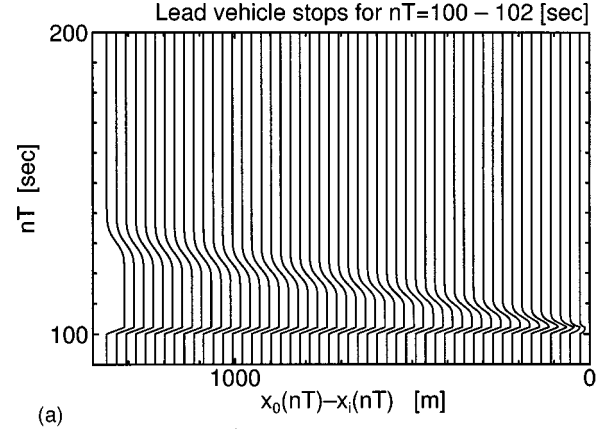


FIG. 5. Numerical simulations for the controlled traffic model. (a) Space-time plot of the controlled traffic model. (b) Temporal velocity behavior of three vehicles.

satisfied, then go to the next step; otherwise, go to exist. (iii) The feedback gains are set as Eq. (27), and then we guarantee condition (24).

This procedure is required for each vehicle. The feedback gains for all the vehicles are designed by the above procedure; then the traffic jam never occurs in the controlled vehicle group.

B. Numerical simulations

Let us suppress the traffic jam by the dynamic version of the DDFC on computer simulations. All the parameters are set as Table I and the other condition is the same as Fig. 2. Now, we shall design the feedback gains to suppress the traffic jam. We know the vehicle parameters ($\alpha_i, v_i^{\max}, \zeta_i, T$), but other information (e.g., the lead-vehicle speed v_0 , vehicle position $x_i(n)$, other vehicle speed, and so on) is not required. For (i), we check that the system parameters satisfy condition (25). For (ii), we confirm that the system parameters satisfy condition (26). For (iii), the feedback gains are designed on the basis of Eq. (27). Figure 5(a) shows the space-time plot of the controlled traffic flow model. We cannot observe the oscillating behavior and the traffic jam phenomena. All the vehicles are running smoothly without full

TABLE II. Ten types of vehicles.

Type	I	II	III	IV	V	VI	VII	VIII	IX	X
α_i	1.8	1.8	1.8	2.0	2.0	2.0	2.0	2.2	2.2	2.2
v_i^{\max}	30	32	34	30	32	33	34	30	32	34
η_i	27	25	23	27	25	23	27	25	23	27

braking. The temporal velocity of the first, 25th, and 50th vehicles is shown in Fig. 5(b). We can see that the minimum speed of the following vehicles decreases with increasing vehicle number i .

The above traffic model consists of identical vehicles: from a practical point of view, such a situation must be a rare case. Let us introduce ten types of vehicles as shown in Table II. Other parameters ζ , T , and y^{\min} are the same as Table I. We consider 100 vehicles consisting of ten different types. For each vehicle the type is selected randomly. Figure 6(a) is the space-time plot of the running traffic model without control. The lead vehicle suddenly stops four times. We observe that the stop disturbances propagate backward. Figure 6(b) shows the speed of the first and 100th vehicles. As you see, the 100th vehicle is running with the maximum speeds v_i^{\max} , stopping for a short time, or oscillating. In order to suppress such unstable behavior, we use the dynamical version of the decentralized delayed-feedback control scheme. The feedback gains for each type are designed by the above systematic procedure. The space-time plot of the running traffic model with control is shown in Figure 7(a). We cannot observe the traffic jam. Figure 7(b) is the speed of the first and 100th vehicles. We can see that the 100th ve-

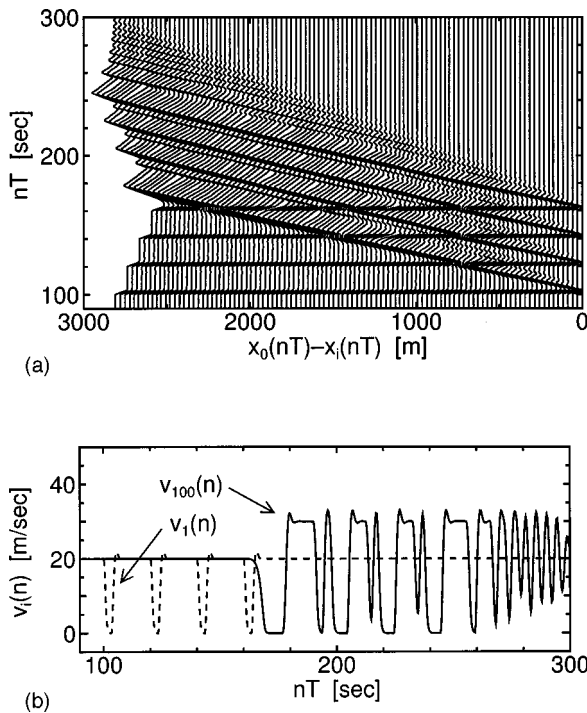


FIG. 6. Numerical simulations for the free-running traffic model consisting of ten type vehicles. The lead-vehicle stops for $nT = 100-103, 120-123, 140-143,$ and $160-163$. (a) Space-time plot of the free-running traffic model. (b) Temporal velocity behavior of the first and 100th vehicles.

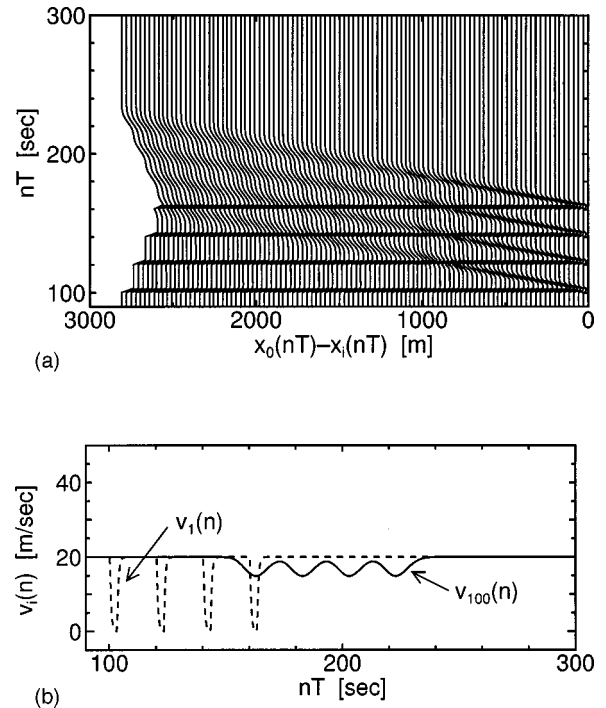


FIG. 7. Numerical simulations for the controlled traffic model consisting of ten type vehicles. The stop of the lead vehicle is the same as Fig. 6. (a) Space-time plot of the controlled traffic model. (b) Temporal velocity behavior of the first and 100th vehicles.

hicle is running smoothly. These numerical simulations show that our control scheme would be a useful method for suppression of a traffic jam.

IV. CONCLUSIONS

This paper proposed the simple CM traffic model describing a dynamical behavior of a group of road vehicles running in a single lane without overtaking. We derived the simple condition under which a traffic jam never occurs in our model. Furthermore, we utilized a dynamical version of the decentralized delayed-feedback control scheme to suppress the traffic jam, and provided a systematic procedure to design the control system. This control scheme for our traffic model has the following four advantages: (i) The controller of each vehicle does not require other vehicle information (e.g., other vehicle speed, vehicle position, vehicle parameters, and so on), (ii) Each controller does not need a desired speed (i.e., the lead vehicle speed), (iii) This control scheme is useful for any size traffic model, and (iv) There is no need to change the vehicle parameters. It is obvious that these advantages are practical for real traffic flows. We showed that numerical simulations agree well with our theoretical results.

We think that our theoretical results would be useful for other load situations: periodic boundary conditions, open boundary bottlenecks, two lanes with overtaking, and so on. It is highly desired to investigate the above situations from practical viewpoints.

ACKNOWLEDGMENTS

This work was partially supported by the Kansai Research Foundation for technology promotion.

APPENDIX A: PROOF OF THEOREM 1

The absolute value of the transfer function $G_i(z)$ can be described as

$$|G_i(z)|_{|z|=1} = \sqrt{\frac{\alpha_i^2 r_i^2 T^4}{g_i(\theta)}} \quad (\text{A1})$$

for all $\theta \in [0, 2\pi]$. The function $g_i(\theta)$ is

$$g_i(\theta) = 4b_i \cos^2 \theta + 2a_i(1+b_i)\cos \theta + (1-b_i)^2 + a_i^2.$$

Condition (18) can be reduced to

$$g_i(\theta) \geq \alpha_i^2 r_i^2 T^4 \quad \forall \theta \in [0, 2\pi] \quad (i=1, 2, \dots, N). \quad (\text{A2})$$

In this proof, we shall derive a simple sufficient condition of Eq. (A2). It is obvious that if the following three conditions,

- (a) $g_i(0) \geq \alpha_i^2 r_i^2 T^4$,
- (b) $\frac{\partial g_i(\theta)}{\partial \theta} \geq 0 \quad \forall \theta \in [0, \pi]$,
- (c) $\frac{\partial g_i(\theta)}{\partial \theta} \leq 0 \quad \forall \theta \in [\pi, 2\pi]$,

are satisfied, then condition (A2) holds.

(a) It is easy to confirm that $g_i(0) = \alpha_i^2 r_i^2 T^4$ for any parameters. Hence, we do not have to consider condition (a).

(b) We have

$$\frac{\partial g_i(\theta)}{\partial \theta} = -2 \sin \theta \{a_i(1+b_i) + 4b_i \cos \theta\} \geq 0 \quad \forall \theta \in [0, \pi]. \quad (\text{A3})$$

Since $-2 \sin \theta \leq 0$ for all $\theta \in [0, \pi]$, we should consider $a_i(1+b_i) + 4b_i \cos \theta \leq 0$ for all $\theta \in [0, \pi]$. As $|\cos \theta| \leq 1$, condition (A3) can be described as

- (i) $a_i(1+b_i) + 4b_i \leq 0$ if $b_i > 0$,
- (ii) $a_i(1+b_i) - 4b_i \leq 0$ if $b_i < 0$,
- (iii) $a_i \leq 0$ if $b_i = 0$.

It is clear that above conditions (i)–(iii) are equal to condition (19).

(c) In a similar manner, we can obtain the same condition as Eq. (19).

APPENDIX B: PROOF OF THEOREM 2

Substituting gains (27) into transfer function (23), we have

$$\bar{G}_i(z) = \frac{\alpha_i r_i T^2 z \left(z - \frac{\alpha_i T(1-r_i T) - 1}{\alpha_i T(1-2r_i T)} \right)}{z^3 \left(z + \frac{r_i T(3 - \alpha_i r_i T^2) - 1}{1 - 2r_i T} \right)}. \quad (\text{B1})$$

Assumption (25) implies that the transfer function $\bar{G}_i(z)$ has no poles outside of unit circle (i.e., stable). It is obvious that if the conditions

- (a) $|G(1)| \leq 1$,
- (b) $|G(e^{j\pi})| \leq 1$,
- (c) $\frac{\partial |G(e^{j\theta})|}{\partial \theta} \neq 0 \quad \forall \theta \in (0, \pi)$,
- (d) $\frac{\partial |G(e^{j\theta})|}{\partial \theta} \neq 0 \quad \forall \theta \in (\pi, 2\pi)$,

are satisfied, then condition (24) holds. (a) It is easy to confirm that $|G(1)| = 1$ for any parameters. (b) Condition (b) can be reduced to

$$\begin{aligned} |G(e^{j\pi})| &= \sqrt{G(e^{j\pi})G(e^{-j\pi})} \\ &= \sqrt{r_i^2 T^2 (1 - 2\alpha_i T + 3\alpha_i r_i T^2)^2 / (2 - 5r_i T + \alpha_i r_i^2 T^3)^2} \leq 1. \end{aligned} \quad (\text{B2})$$

We see that condition (b) is always satisfied under assumption (26). (c) Substituting $e^{j\theta} = \cos \theta + j \sin \theta$ into condition (c), we can prove that condition (c) always holds. (d) In a similar manner, we can prove that condition (d) always holds.

[1] G. Chen and X. Dong, *From Chaos to Order* (World Scientific, Singapore, 1998).
 [2] E. Ott, C. Grebogi, and J. A. Yorke, *Phys. Rev. Lett.* **64**, 1196 (1990).
 [3] K. Pyragas, *Phys. Lett. A* **170**, 421 (1992).
 [4] M. E. Bleich and J. E. S. Socolar, *Phys. Lett. A* **210**, 87 (1996).
 [5] W. Just *et al.*, *Phys. Rev. Lett.* **78**, 203 (1997).
 [6] H. Nakajima, *Phys. Lett. A* **232**, 207 (1997).
 [7] H. Kokame and T. Mori (unpublished).
 [8] S. Bielawski, D. Derozier, and P. Glorieux, *Phys. Rev. A* **47**, R2492 (1993).
 [9] T. Ushio, *IEEE Trans. Circuits Syst., I: Fundam. Theory Appl.* **43**, 815 (1996).

[10] M. de Sousa Vieira and A. J. Lichtenberg, *Phys. Rev. E* **54**, 1200 (1996).
 [11] M. Ishii, K. Konishi, and H. Kokame, *Phys. Lett. A* **235**, 603 (1997).
 [12] K. Konishi, M. Ishii, and H. Kokame, *Phys. Rev. E* **54**, 3455 (1996).
 [13] K. Konishi, M. Ishii, and H. Kokame, *IEEE Trans. Circuits Syst., I: Fundam. Theory Appl.* (to be published).
 [14] G. Hu, Z. Qu, and K. He, *Int. J. Bifurcation Chaos Appl. Sci. Eng.* **5**, 901 (1997).
 [15] K. Konishi, M. Hirai, and H. Kokame, *Phys. Rev. E* **58**, 3055 (1998).
 [16] F. H. Willeboordse and K. Kaneko, *Phys. Rev. Lett.* **73**, 533 (1994).

- [17] F. H. Willeboordse and K. Kaneko, *Physica D* **86**, 428 (1995).
- [18] M. Bando *et al.*, *Phys. Rev. E* **51**, 1035 (1995).
- [19] T. S. Komatsu and S. Sasa, *Phys. Rev. E* **52**, 5574 (1995).
- [20] M. Bando *et al.*, *Phys. Rev. E* **58**, 5429 (1998).
- [21] T. Nagatani and K. Nakanishi, *Phys. Rev. E* **57**, 6415 (1998).
- [22] K. Nakanishi *et al.*, *Phys. Rev. E* **55**, 6519 (1997).
- [23] Y. Sugiyama and H. Yamada, *Phys. Rev. E* **55**, 7749 (1997).
- [24] H. Hayakawa and K. Nakanishi, *Phys. Rev. E* **57**, 3839 (1998).
- [25] P. S. Addison and D. J. Low, *Chaos* **8**, 791 (1998).
- [26] S. Yukawa and M. Kikuchi, *J. Phys. Soc. Jpn.* **64**, 35 (1995).
- [27] S. Yukawa and M. Kikuchi, *J. Phys. Soc. Jpn.* **65**, 916 (1996).
- [28] S. Tadaki *et al.*, *J. Phys. Soc. Jpn.* **67**, 2270 (1998).
- [29] O. Biham, A. A. Middleton, and D. Levine, *Phys. Rev. A* **46**, R6124 (1992).
- [30] S. Yukawa, M. Kikuchi, and S. Tadaki, *J. Phys. Soc. Jpn.* **63**, 3609 (1994).
- [31] K. Nagel *et al.*, *Phys. Rev. E* **58**, 1425 (1998).
- [32] P. M. Simon and K. Nagel, *Phys. Rev. E* **58**, 1286 (1998).